Amplitude reduction at two loops

Costas G. Papadopoulos

in collaboration with
G. Bevilacqua, D. Canko, A. Spourdalakis

INPP, NCSR "Demokritos", 15310 Athens, Greece

HOCTools-II

9th annual Xmas Theoretical Physics Workshop, 18-20 December 2024

Outline

1. Introduction: what calculations we need
2. LO: from Feynman diagrams to recursive equations
3. The NLO revolution: from Feynman Integrals to integrands
4. Towards higher precision: NNLO
   - Constructing the 2-loop integrand $\rightarrow$ NNLO
   - Integrand reduction: $d = 4$ versus $d = 4 - 2\epsilon$ $\rightarrow$ NLO & NNLO
5. Summary - Discussion

Higgs

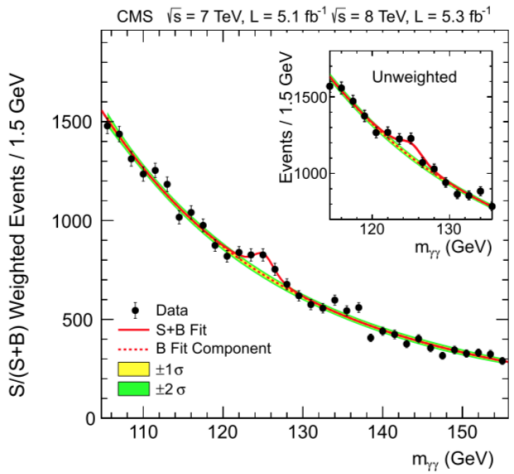

Fig. 3. The diphoton invariant mass distribution with each event weighted by the $S/(S+B)$ value of its category. The lines represent the fitted background and signal, and the coloured bands represent the ± 1 and ± 2 standard deviation uncertainties in the background estimate. The inset shows the central part of the unweighted invariant mass distribution. (For interpretation of the references to colour in this figure legend, the reader is referred to the web version of this Letter.)

Gravitational wave

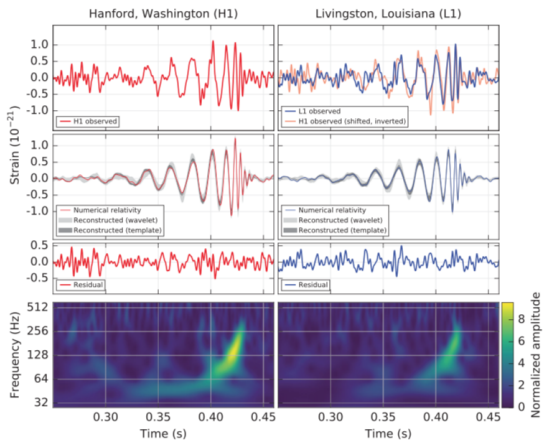

FIG. 1. The gravitational-wave event GW150914 observed by the LIGO Hanford (H1, left column panels) and Livingston (L1, right column panels) detectors. Times are shown relative to September 14, 2015 at 09:50:45 UTC. For visualization, all time series are filtered with a 35–350 Hz bandpass filter to suppress large fluctuations outside the detectors' most sensitive frequency band, and band-reject filters to remove the strong instrumental spectral lines seen in the Fig. 3 spectra. *Top row, left:* H1 strain. *Top row, right:* L1 strain. GW150914 arrived first at L1 and $6.9^{+0.5}_{-0.4}$ ms later at H1; for a visual comparison, the H1 data are also shown, shifted in time by this amount and inverted (to account for the detectors' relative orientations). *Second row:* Gravitational-wave strain projected onto each detector in the 35–350 Hz band. Solid lines show a numerical relativity waveform for a system with parameters consistent with those recovered from GW150914 [37,38] confirmed to 99.9% by an independent calculation based on [15]. Shaded areas show 90% credible regions for two independent waveform reconstructions. One (dark gray) models the signal using binary black hole template waveforms [39]. The other (light gray) does not use an astrophysical model, but instead calculates the strain signal as a linear combination of sine-Gaussian wavelets [40,41]. These reconstructions have a 94% overlap, as shown in [39]. *Third row:* Residuals after subtracting the filtered numerical relativity waveform from the filtered detector time series. *Bottom row:* A time-frequency representation [42] of the strain data, showing the signal frequency increasing over time.

BH Horizon

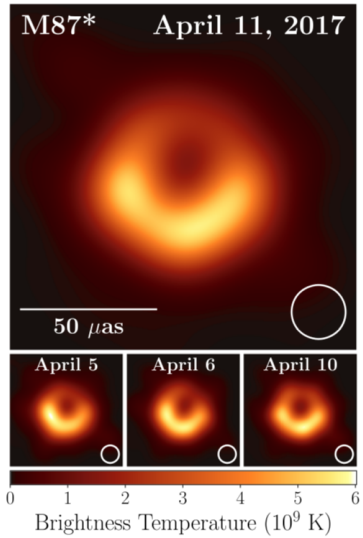

Figure 3. Top: EHT image of M87* from observations on 2017 April 11 as a representative example of the images collected in the 2017 campaign. The image is the average of three different imaging methods after convolving each with a circular Gaussian kernel to give matched resolutions. The largest of the three kernels (20 μas FWHM) is shown in the lower right. The image is shown in units of brightness temperature, $T_b = S\lambda^2/2k_B\Omega$, where S is the flux density, λ is the observing wavelength, k_B is the Boltzmann constant, and Ω is the solid angle of the resolution element. Bottom: similar images taken over different days showing the stability of the basic image structure and the equivalence among different days. North is up and east is to the left.

INTRODUCTION

LHC

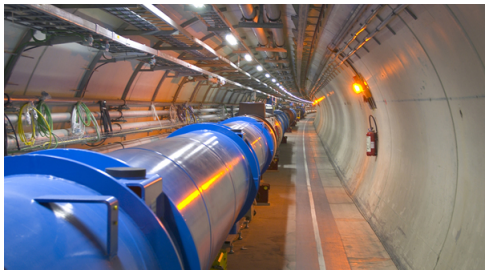

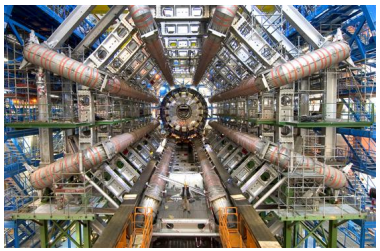

LIGO

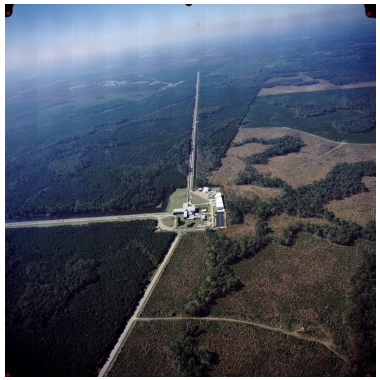

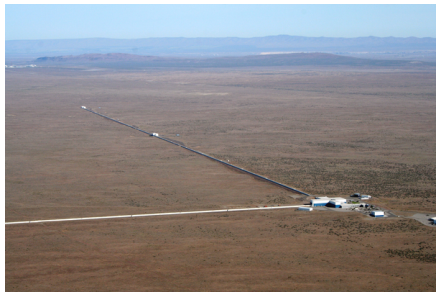

EHT

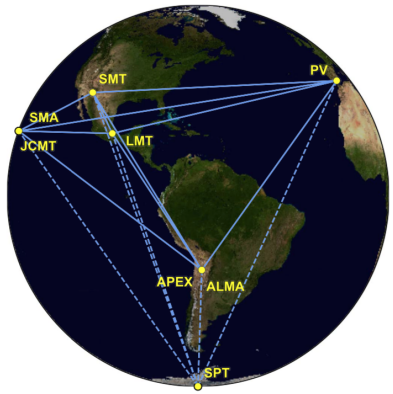

Figure 1. Eight stations of the EHT 2017 campaign over six geographic locations as viewed from the equatorial plane. Solid baselines represent mutual visibility on M87° (+12° declination). The dashed baselines were used for the calibration source 3C279 (see Papers III and IV).

INTRODUCTION

LHC

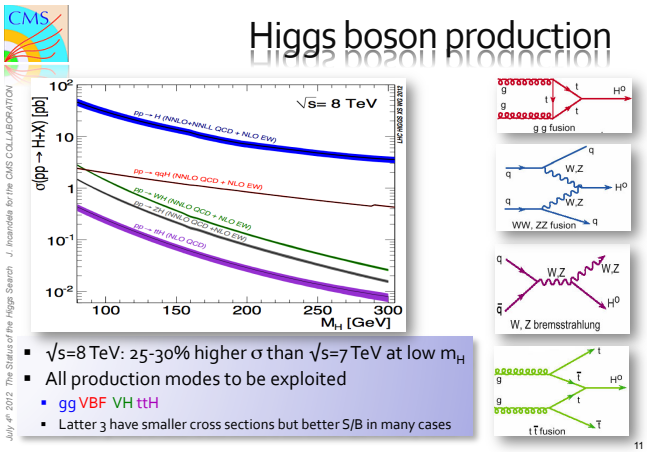

LIGO

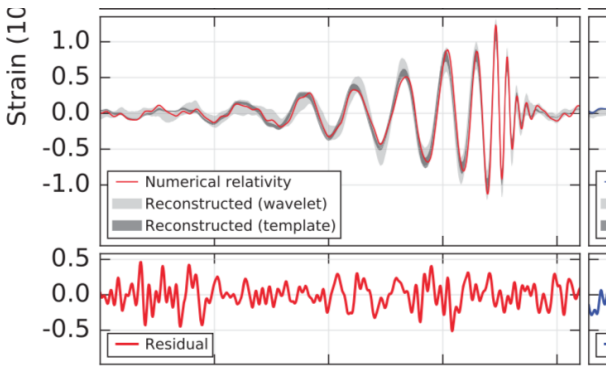

EHT

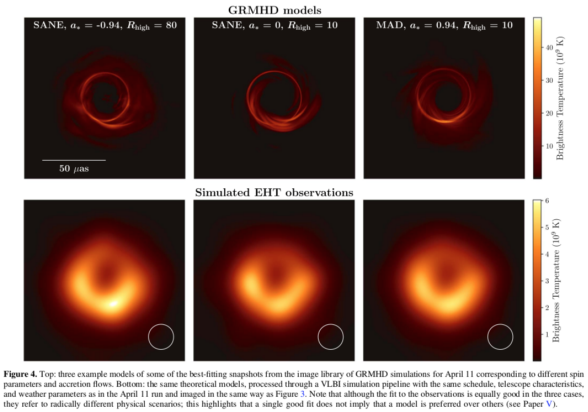

Figure 4. Top: three example models of some of the best-fitting snapshots from the image library of GRMHD simulations for April 11 corresponding to different spin parameters and accretion flows. Bottom: the same theoretical models, processed through a VLBI simulation pipeline with the same schedule, telescope characteristics, and weather parameters as in the April 11 run and imaged in the same way as Figure 3. Note that although the fit to the observations is equally good in the three cases, they refer to radically different physical scenarios; this highlights that a single good fit does not imply that a model is preferred over others (see Paper V).

Faint signals; Patience; Theory

LHC SCHEDULE

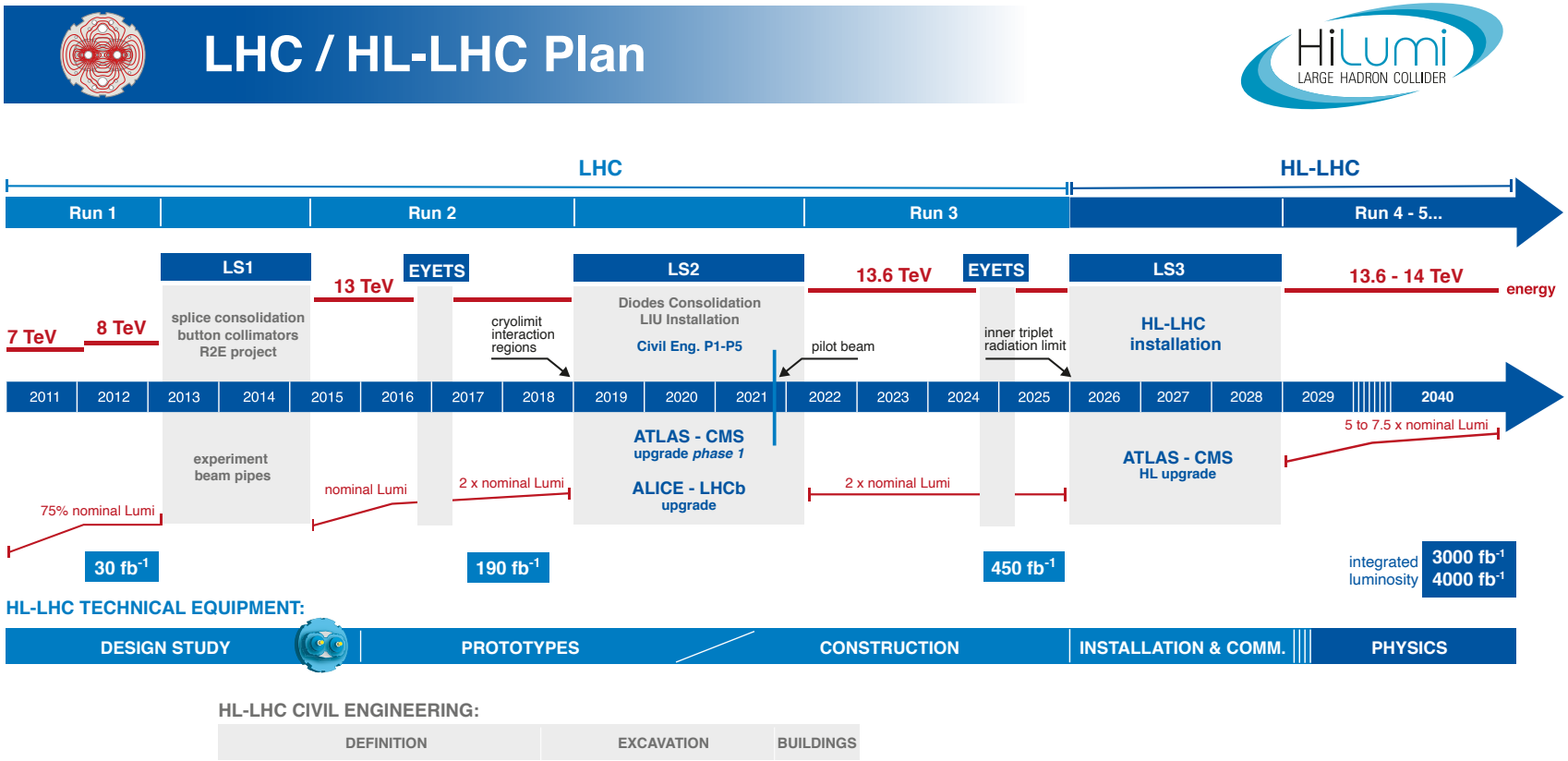

LHC PRECISION

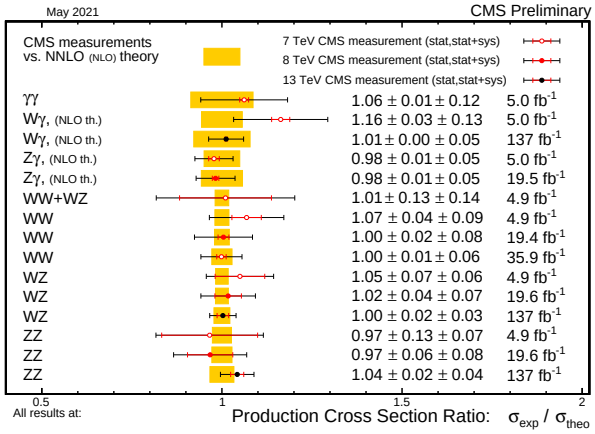

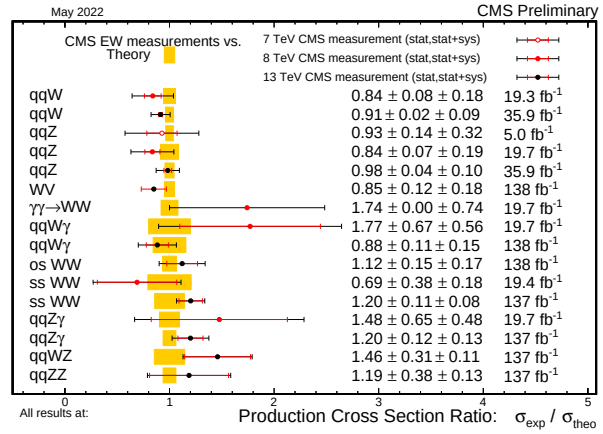

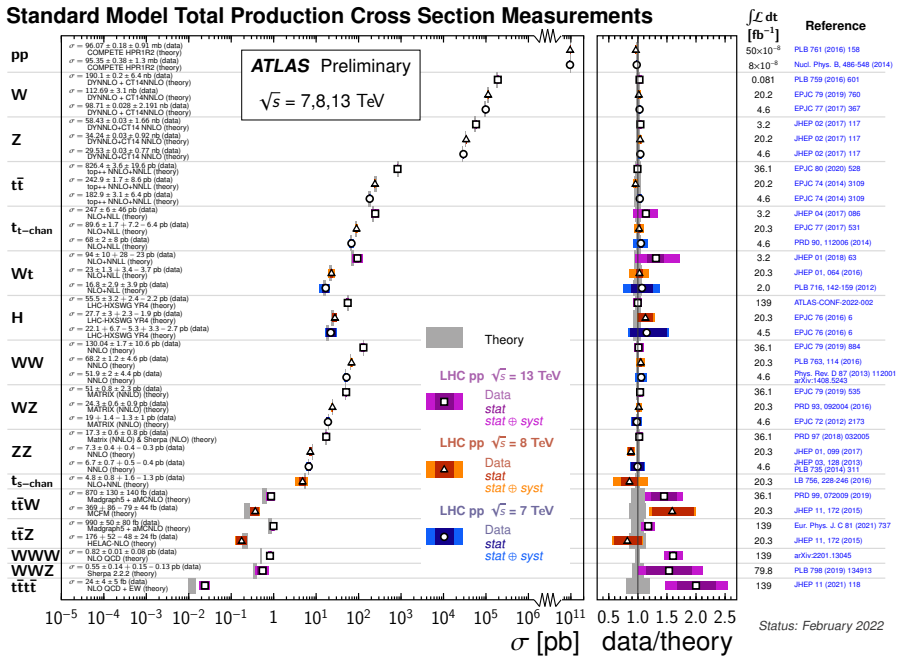

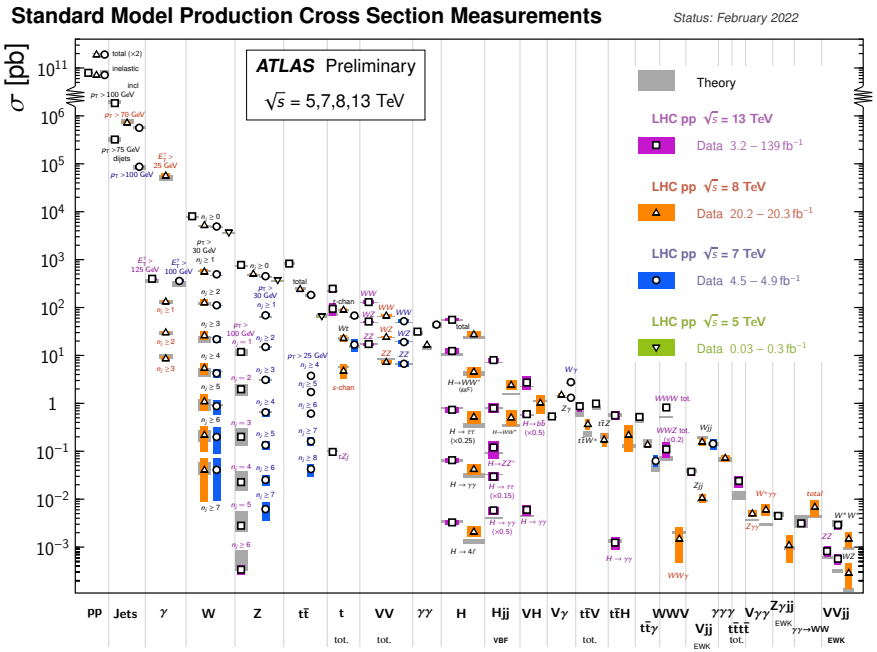

Improved theoretical predictions are indispensable

FCC

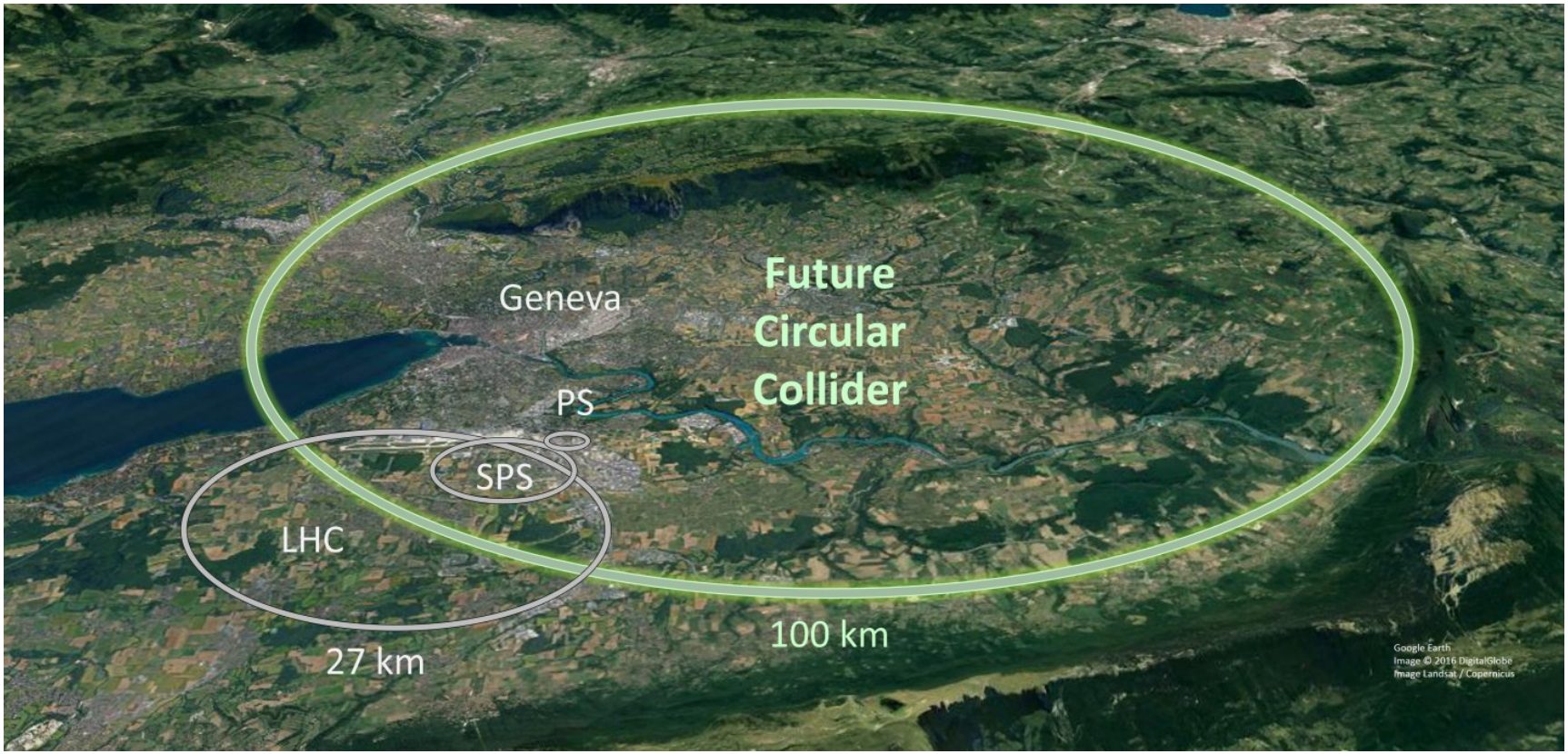

circular accelerators with decelerating pace of expansion!

FCC-hh rates - Higgs

→ A. Abada *et al.* [FCC], Eur. Phys. J. ST **228** (2019) no.4, 755-1107

Table 1.1: Higgs production event rates for selected processes at 100 TeV (N_{100}) and statistical increase with respect to the statistics of the HL-LHC ($N_{100} = \sigma_{100\ \mathrm{TeV}} \times 30\ \mathrm{ab}^{-1}$, $N_{14} = \sigma_{14\ \mathrm{TeV}} \times 3\ \mathrm{ab}^{-1}$).

	$gg \to H$	VBF	WH	ZH	$t\bar{t}H$	HH
N_{100}	24×10^9	2.1×10^9	4.6×10^8	3.3×10^8	9.6×10^8	3.6×10^7
N_{100}/N_{14}	180	170	100	110	530	390

FCC-hh RATES - TOP

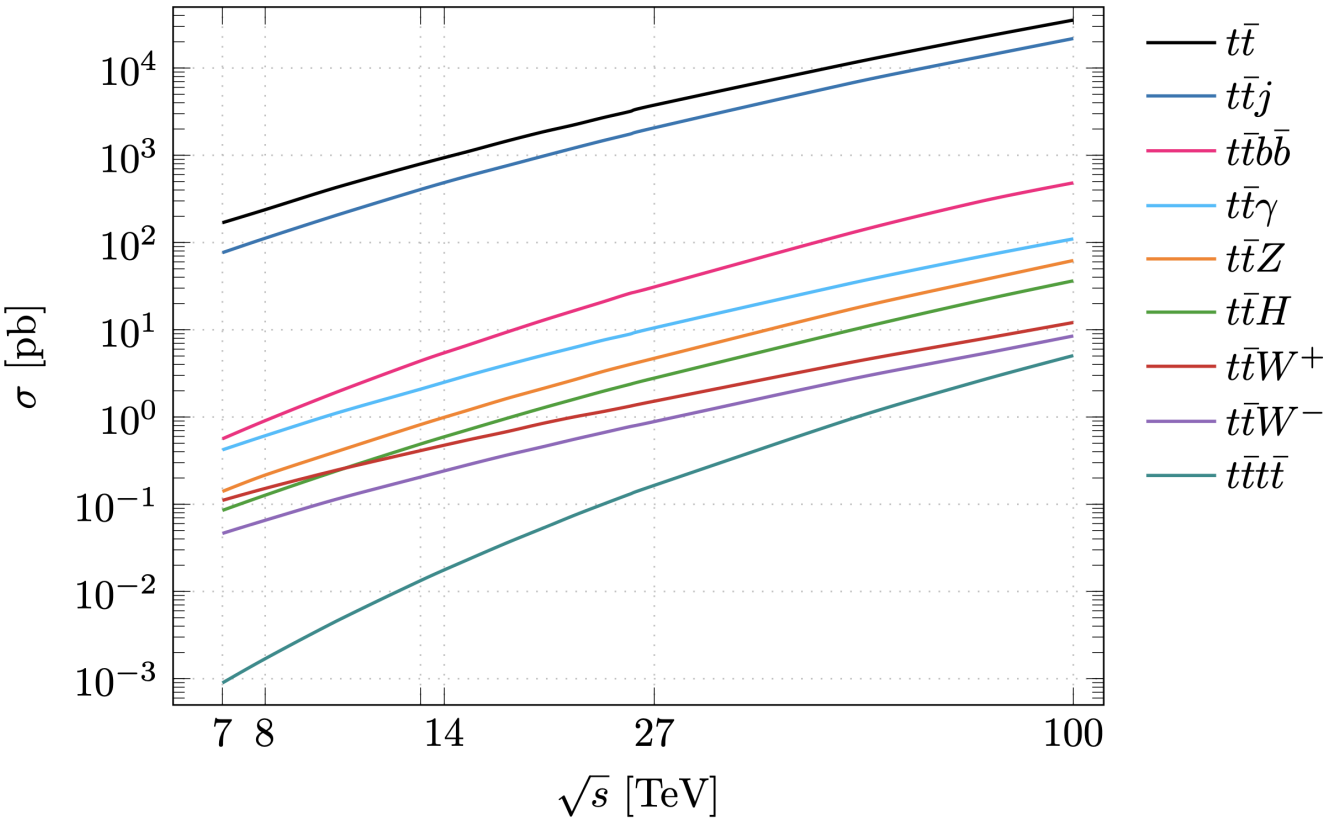

Courtesy of Manfred Kraus/Malgorzata Worek

FCC-ee rates

→ A. Blondel, *et al.* [arXiv:1905.05078 [hep-ph]].

TABLE: Run plan for FCC-ee in its baseline configuration with two experiments. The WW event numbers are given for the entirety of the FCC-ee running at and above the WW threshold.

Phase	Run duration (years)	Centre-of-mass energies (GeV)	Integrated luminosity (ab^{-1})	Event statistics
FCC-ee-Z	4	88–95	150	3×10^{12} visible Z decays
FCC-ee-W	2	158–162	12	10^8 WW events
FCC-ee-H	3	240	5	10^6 ZH events
FCC-ee-tt	5	345–365	1.5	10^6 $t\bar{t}$ events

Fixed-order calculations

Factorization

Collins,Soper,Sterman'85–'89

- Calculate
  - Scattering probability
  - Gluon emission probability
- Measure
  - Long distance interactions
  - Particle decay rates

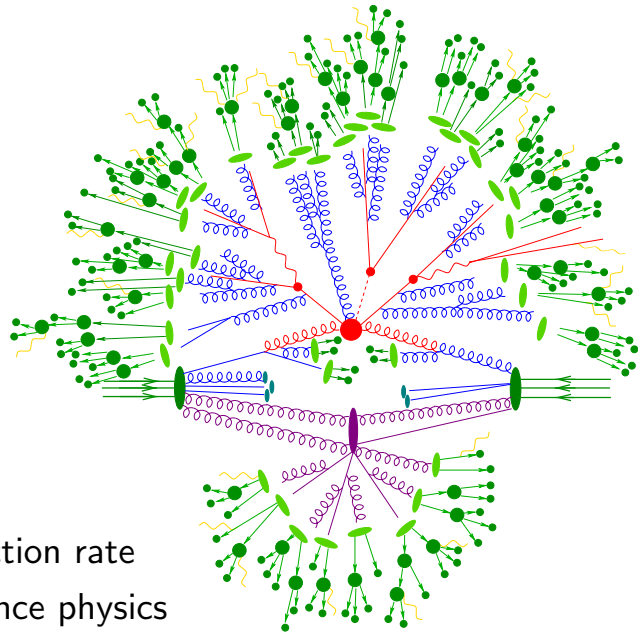

Divide et Impera

- Quantity of interest: Total interaction rate
- Convolution of short & long distance physics

$$\sigma_{p_1 p_2 \to X} = \sum_{i,j \in \{q,g\}} \int \mathrm{d}x_1 \mathrm{d}x_2 \underbrace{f_{p_1,i}(x_1,\mu_F^2) f_{p_2,j}(x_2,\mu_F^2)}_{\text{long distance physics}} \underbrace{\hat{\sigma}_{ij\to X}(x_1 x_2, \mu_F^2)}_{\text{short distance physics}}$$

QCD as a perturbative quantum field theory

Factorization

Collins,Soper,Sterman'85–'89

- Calculate
  - Scattering probability
  - Gluon emission probability
- Measure
  - Long distance interactions
  - Particle decay rates

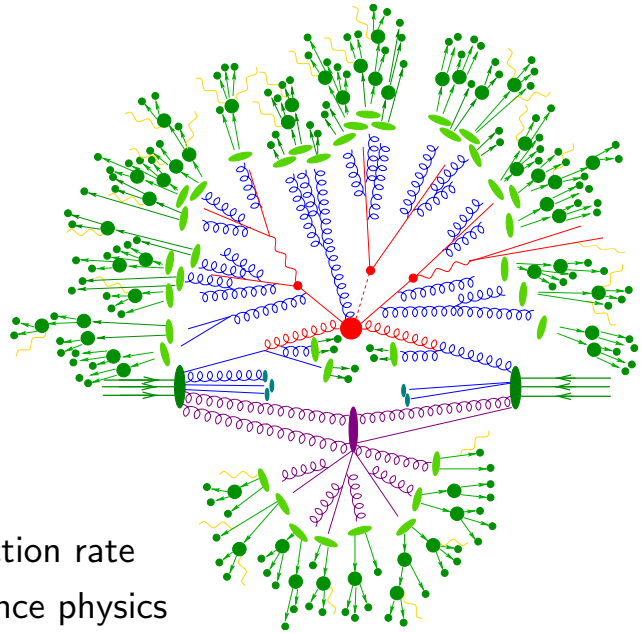

Divide et Impera

- Quantity of interest: Total interaction rate
- Convolution of short & long distance physics

$$\sigma_{p_1 p_2 \to X} = \sum_{i,j \in \{q,g\}} \int \mathrm{d}x_1 \mathrm{d}x_2 \underbrace{f_{p_1,i}(x_1,\mu_F^2) f_{p_2,j}(x_2,\mu_F^2)}_{\text{long distance physics}} \underbrace{\hat{\sigma}_{ij\to X}(x_1 x_2, \mu_F^2)}_{\text{short distance physics}}$$

QCD as a perturbative quantum field theory

Lattice QCD results:

→ C. Alexandrou, *et al.* Phys. Rev. Lett. **121**, 112001 (2018) [arXiv:1803.02685 [hep-lat]].

DS recursive equations

How to avoid Feynman diagrams

$\rightarrow$ a highly subjective point of view

LO - Dyson-Schwinger Recursive Equations

From Feynman Diagrams to recursive equations: taming the $n!$

- 1999 HELAC: The first code to calculate recursively tree-order amplitudes for (practically) arbitrary number of particles

→A. Kanaki and C. G. Papadopoulos, Comput. Phys. Commun. **132** (2000) 306 [arXiv:hep-ph/0002082].

→F. A. Berends and W. T. Giele, Nucl. Phys. B **306** (1988) 759.

→ F. Caravaglios and M. Moretti, Phys. Lett. B **358** (1995) 332.

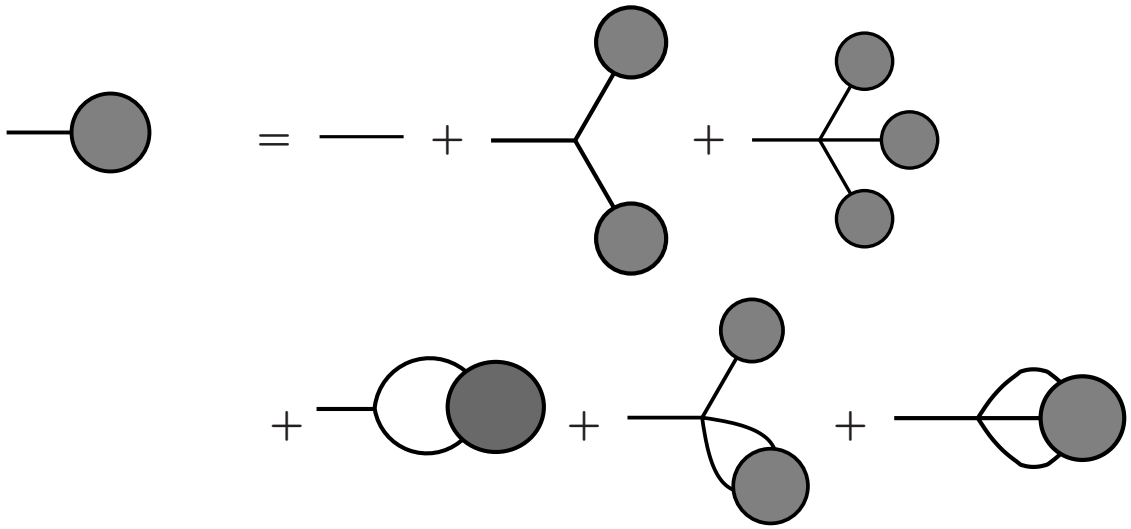

Unfortunately not so much on the second line !

→Integrals and Integrands

Taming the beast ...

From Feynman graphs ...

$gg \to ng$	2	3	4	5	6	7	8	9
# FG	4	25	220	2,485	34,300	559,405	10,525,900	224,449,225

to Dyson-Schwinger recursion! `Helac-Phegas`

$gg \to ng$	2	3	4	5	6	7	8	9
#	5	15	35	70	126	210	330	495

Beyond tree-order

NLO

Don't make integrals, make integrands !

basis of scalar integrals: known already before NLO-R; remember this is not the case for higher orders

→G. 't Hooft and M. J. G. Veltman, Nucl. Phys. B **153** (1979) 365.

→ Z. Bern, L. J. Dixon and D. A. Kosower, Nucl. Phys. B **412** (1994) 751

→G. Passarino and M. J. G. Veltman, Nucl. Phys. B **160** (1979) 151.

→Z. Bern, L. J. Dixon, D. C. Dunbar and D. A. Kosower, Nucl. Phys. B **425** (1994) 217.

$$\mathcal{A} = \sum_{I\subset\{0,1,\cdots,m-1\}} \int \frac{\mu^{(4-d)} d^d\bar{q}}{(2\pi)^d} \frac{\bar{N}_I(\bar{q})}{\prod_{i\in I}\bar{D}_i(\bar{q})}$$

$$\mathcal{A} = \sum d_{i_1 i_2 i_3 i_4}$$ 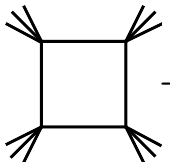 $$+ \sum c_{i_1 i_2 i_3}$$ 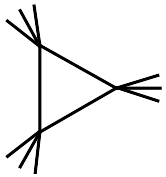 $$+ \sum b_{i_1 i_2}$$ 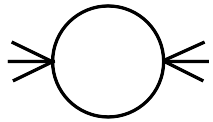 $$+ \sum a_{i_1}$$ 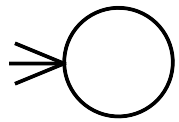 $$+ R$$

$a, b, c, d \rightarrow$ cut-constructible part $\qquad R \rightarrow$ rational terms

The old "master" formula

$$\mathcal{A} \to \int \frac{\bar{N}(\bar{q})}{\bar{D}_0 \bar{D}_1 \cdots \bar{D}_{m-1}} = \sum_{i_0<i_1<i_2<i_3}^{m-1} d(i_0 i_1 i_2 i_3) \int \frac{1}{\bar{D}_{i0} \bar{D}_{i1} \bar{D}_{i2} \bar{D}_{i2}}$$
$$+ \sum_{i_0<i_1<i_2}^{m-1} c(i_0 i_1 i_2) \int \frac{1}{\bar{D}_{i0} \bar{D}_{i1} \bar{D}_{i2}}$$
$$+ \sum_{i_0<i_1}^{m-1} b(i_0 i_1) \int \frac{1}{\bar{D}_{i0} \bar{D}_{i1}}$$
$$+ \sum_{i_0}^{m-1} a(i_0) \int \frac{1}{\bar{D}_{i0}}$$
$$+ \text{rational terms}$$

OPP "master" formula - I

General expression for the 4-dim $N(q)$ at the integrand level in terms of D_i

→ G. Ossola, C. G. Papadopoulos and R. Pittau, [arXiv:hep-ph/0609007 [hep-ph]].

$$
\begin{aligned}
N(q) \;=\; & \sum_{i_0<i_1<i_2<i_3}^{m-1} \left[d(i_0 i_1 i_2 i_3) + \tilde{d}(q; i_0 i_1 i_2 i_3) \right] \prod_{i\neq i_0,i_1,i_2,i_3}^{m-1} D_i \\
+ & \sum_{i_0<i_1<i_2}^{m-1} \left[c(i_0 i_1 i_2) + \tilde{c}(q; i_0 i_1 i_2) \right] \prod_{i\neq i_0,i_1,i_2}^{m-1} D_i \\
+ & \sum_{i_0<i_1}^{m-1} \left[b(i_0 i_1) + \tilde{b}(q; i_0 i_1) \right] \prod_{i\neq i_0,i_1}^{m-1} D_i \\
+ & \sum_{i_0}^{m-1} \left[a(i_0) + \tilde{a}(q; i_0) \right] \prod_{i\neq i_0}^{m-1} D_i
\end{aligned}
$$

OPP R_1

→G. Ossola, C. G. Papadopoulos and R. Pittau, JHEP **05** (2008), 004 [arXiv:0802.1876 [hep-ph]].

$$\bar{D}_i = (\bar{q} + p_i)^2 - m_i^2 \,, \quad p_0 \neq 0 \,,$$

$$\bar{D}_i = D_i + \tilde{q}^2$$

$$m_i^2 \to m_i^2 - \tilde{q}^2 .$$

$$\begin{aligned} d(ijkl;\tilde{q}^2) &= d(ijkl) + \tilde{q}^2 d^{(2)}(ijkl) + \tilde{q}^4 d^{(4)}(ijkl) \,, \\ c(ijk;\tilde{q}^2) &= c(ijk) + \tilde{q}^2 c^{(2)}(ijk) \,, \\ b(ij;\tilde{q}^2) &= b(ij) + \tilde{q}^2 b^{(2)}(ij) \,. \end{aligned}$$

$$
\begin{aligned}
d^{(4)}(ijkl) &= \lim_{\tilde{q}^2\to\infty} \frac{d(ijkl;\tilde{q}^2)}{\tilde{q}^4}\,, \\
c^{(2)}(ijk) &= \lim_{\tilde{q}^2\to\infty} \frac{c(ijk;\tilde{q}^2)}{\tilde{q}^2}\,, \\
b^{(2)}(ij) &= \lim_{\tilde{q}^2\to\infty} \frac{b(ij;\tilde{q}^2)}{\tilde{q}^2}\,,
\end{aligned}
$$

$$
\begin{aligned}
d^{(4)}(ijkl) &= \frac{d(ijkl;1)+d(ijkl;-1)-2d(ijkl)}{2}\,, \\
c^{(2)}(ijk) &= c(ijk;1)-c(ijk)\,, \\
b^{(2)}(ij) &= b(ij;1)-b(ij)\,.
\end{aligned}
$$

OPP R_1

$$\int d^n\bar{q}\frac{\tilde{q}^4}{\bar{D}_i\bar{D}_j\bar{D}_k\bar{D}_l} = -\frac{i\pi^2}{6}+\mathcal{O}(\epsilon)\,,$$

$$\int d^n\bar{q}\frac{\tilde{q}^2}{\bar{D}_i\bar{D}_j\bar{D}_k} = -\frac{i\pi^2}{2}+\mathcal{O}(\epsilon)\,,$$

$$\int d^n\bar{q}\frac{\tilde{q}^2}{\bar{D}_i\bar{D}_j} = -\frac{i\pi^2}{2}\left[m_i^2+m_j^2-\frac{(p_i-p_j)^2}{3}\right]+\mathcal{O}(\epsilon)\,.$$

OPP R_1

$$
\begin{aligned}
\mathrm{R}_1 \;=\; & -\frac{i}{96\pi^2}\, d^{(2m-4)} - \frac{i}{32\pi^2} \sum_{i_0<i_1<i_2}^{m-1} c^{(2)}(i_0 i_1 i_2) \\
- \; & \frac{i}{32\pi^2} \sum_{i_0<i_1}^{m-1} b^{(2)}(i_0 i_1) \left(m_{i_0}^2 + m_{i_1}^2 - \frac{(p_{i_0} - p_{i_1})^2}{3} \right) .
\end{aligned}
$$

OPP R_2

→P. Draggiotis, M. V. Garzelli, C. G. Papadopoulos and R. Pittau, JHEP **04** (2009), 072 [arXiv:0903.0356 [hep-ph]].

→ M. V. Garzelli, I. Malamos and R. Pittau, JHEP **01** (2010), 040 [erratum: JHEP **10** (2010), 097]

$$\bar{N}(\bar{q}) = N(q) + \tilde{N}(\tilde{q}^2, q, \epsilon)\,.$$

$$\begin{aligned} \bar{q} &= q + \tilde{q}\,, \\ \bar{\gamma}_{\bar{\mu}} &= \gamma_\mu + \tilde{\gamma}_{\tilde{\mu}}\,, \\ \bar{g}^{\bar{\mu}\bar{\nu}} &= g^{\mu\nu} + \tilde{g}^{\tilde{\mu}\tilde{\nu}}\,. \end{aligned}$$

$$\mathrm{R}_2 \equiv \frac{1}{(2\pi)^4} \int d^n\,\bar{q}\, \frac{\tilde{N}(\tilde{q}^2, q, \epsilon)}{\bar{D}_0 \bar{D}_1 \cdots \bar{D}_{m-1}} \equiv \frac{1}{(2\pi)^4} \int d^n\,\bar{q}\, \mathcal{R}_2\,.$$

OPP R_2

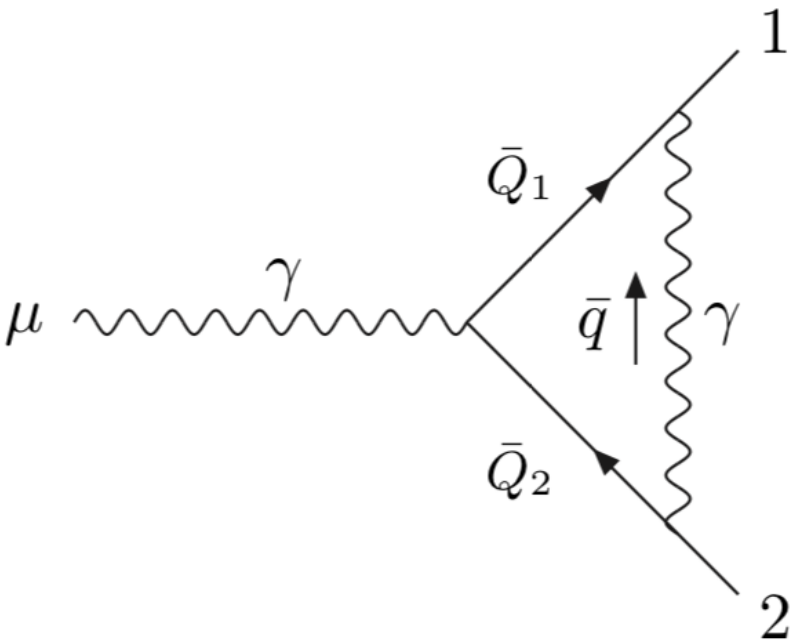

$$\bar{Q}_1 = \bar{q} + p_1 = Q_1 + \tilde{q}$$
$$\bar{Q}_2 = \bar{q} + p_2 = Q_2 + \tilde{q}$$

$$\bar{D}_0 = \bar{q}^2$$
$$\bar{D}_1 = (\bar{q} + p_1)^2$$
$$\bar{D}_2 = (\bar{q} + p_2)^2$$

Figure 1: QED $\gamma e^+ e^-$ diagram in n dimensions.

OPP R_2

ϵ-dimensional γ matrices freely anti-commute with four-dimensional ones: $\{\gamma_\mu, \tilde{\gamma}_\nu\} = 0$

$$\begin{aligned}
\bar{N}(\bar{q}) &\equiv e^3 \left\{ \bar{\gamma}_{\bar{\beta}} \left(\bar{\not{Q}}_1 + m_e\right) \gamma_\mu \left(\bar{\not{Q}}_2 + m_e\right) \bar{\gamma}^{\bar{\beta}} \right\} \\
&= e^3 \left\{ \gamma_\beta (\not{Q}_1 + m_e) \gamma_\mu (\not{Q}_2 + m_e) \gamma^\beta \right. \\
&- \left. \epsilon\, (\not{Q}_1 - m_e) \gamma_\mu (\not{Q}_2 - m_e) + \epsilon \tilde{q}^2\, \gamma_\mu - \tilde{q}^2\, \gamma_\beta \gamma_\mu \gamma^\beta \right\} ,
\end{aligned}$$

$$\begin{aligned}
\int d^n \bar{q} \frac{\tilde{q}^2}{\bar{D}_0 \bar{D}_1 \bar{D}_2} &= -\frac{i\pi^2}{2} + \mathcal{O}(\epsilon) , \\
\int d^n \bar{q} \frac{q_\mu q_\nu}{\bar{D}_0 \bar{D}_1 \bar{D}_2} &= -\frac{i\pi^2}{2\epsilon} g_{\mu\nu} + \mathcal{O}(1) ,
\end{aligned}$$

gives

$$\mathrm{R}_2 = -\frac{ie^3}{8\pi^2} \gamma_\mu + \mathcal{O}(\epsilon) ,$$

OPP R_2

Computing 1PI contributions to $R_2 \to R_2$ for any 1-loop amplitude

R_2 vertices in full analogy with renormalization CT

OPP@work

1. Determining the on-shell momenta through $D_i = 0$ and computing all coefficients.
2. Determining the on-shell momenta through $D_i = \mu$ and μ dependence of certain coefficients, namely R_1.
3. Using new Feynman rules to compute with tree-like DS the rest of R contribution, namely R_2.

→ G. Ossola, C. G. Papadopoulos and R. Pittau, [arXiv:0802.1876 [hep-ph]].

→ M. V. Garzelli, I. Malamos and R. Pittau, [arXiv:0910.3130 [hep-ph]].

Towards higher precision:

NNLO and beyond

I have a dream ...

What do we need for an NNLO calculation ?

$$p_1, p_2 \to p_3, \ldots, p_{m+2}$$

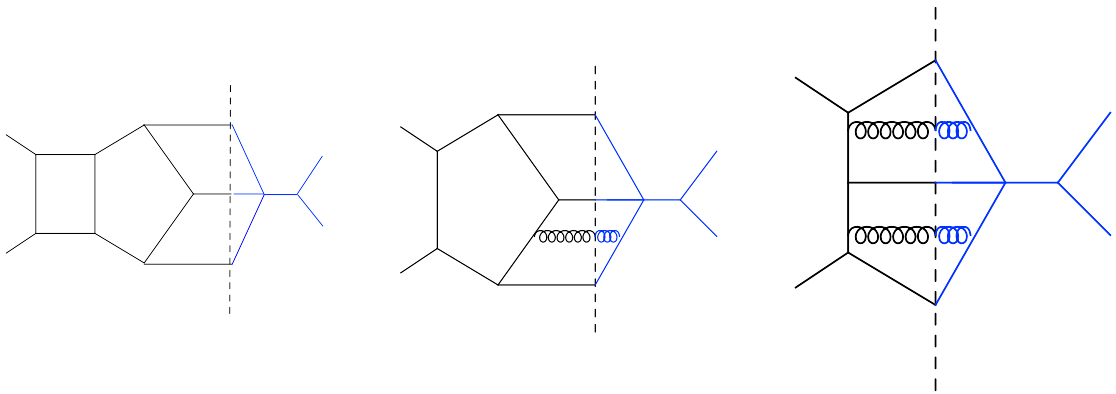

What do we need for an NNLO calculation ?

$$\sigma_{NNLO} \rightarrow \int_m d\Phi_m \left(2Re(M_m^{(0)*} M_m^{(2)}) + \left| M_m^{(1)} \right|^2 \right) J_m(\Phi) \qquad VV$$

$$+ \int_{m+1} d\Phi_{m+1} \left(2Re \left(M_{m+1}^{(0)*} M_{m+1}^{(1)} \right) \right) J_{m+1}(\Phi) \qquad RV$$

$$+ \int_{m+2} d\Phi_{m+2} \left| M_{m+2}^{(0)} \right|^2 J_{m+2}(\Phi) \qquad RR$$

$RV + RR \rightarrow$ `antenna-S`, `colorfull-NNLO`, `sector-improved residue subtraction`, `nested soft-collinear`, `local analytic sector subtraction`, `projection to born`, q_T, N-jetiness

→A. Gehrmann-De Ridder, T. Gehrmann and M. Ritzmann, JHEP **1210** (2012) 047

→ P. Bolzoni, G. Somogyi and Z. Trocsanyi, JHEP **1101** (2011) 059

→ M. Czakon and D. Heymes, Nucl. Phys. B **890** (2014) 152

→S. Catani and M. Grazzini, Phys. Rev. Lett. **98** (2007) 222002

→ R. Boughezal, C. Focke, X. Liu and F. Petriello, Phys. Rev. Lett. **115** (2015) no.6, 062002

→ M. Cacciari, F. A. Dreyer, A. Karlberg, G. P. Salam and G. Zanderighi, Phys. Rev. Lett. **115**, no. 8, 082002 (2015)

→ F. Caola, K. Melnikov and R. Röntsch, Eur. Phys. J. C **77**, no. 4, 248 (2017)

→ L. Magnea, E. Maina, G. Pelliccioli, C. Signorile-Signorile, P. Torrielli and S. Uccirati, arXiv:1806.09570 [hep-ph].

Amplitude construction

Amplitude construction

- Standard approach: QGRAF → symbolic manipulation, dimensionally regularized amplitudes → IBP: `FIRE`, `Kira` or numerical `pySecDec`

- Numerical unitarity → dimensionally regularized amplitudes by gluing tree amplitudes in different integer dimensions → D_s

  → S. Abreu, J. Dormans, F. Febres Cordero, H. Ita, M. Kraus, B. Page, E. Pascual, M. S. Ruf and V. Sotnikov, CPC **267** (2021), 108069

- OpenLoops → Feynman graph → opening the loops → amplitudes in $d = 4$ → coefficients of tensor integrals

  → S. Pozzorini, N. Schär and M. F. Zoller, [arXiv:2201.11615 [hep-ph]].

  → talk by Max Zoller

Colour flow or colour connection representation

$$\mathcal{M}^{a_1,i_2,\ldots,i_k}_{j_2,\ldots,j_k}\, t^{a_1}_{i_1 j_1} \to \mathcal{M}^{i_1,i_2,\ldots,i_k}_{j_1,j_2,\ldots,j_k}$$

$$\mathcal{M}^{i_1,i_2,\ldots,i_k}_{j_1,j_2,\ldots,j_k} = \sum_{\sigma} \delta_{i_{\sigma_1},j_1}\delta_{i_{\sigma_2},j_2}\ldots\delta_{i_{\sigma_k},j_k} A_\sigma \to n!$$

gluons, ghosts $\to (i,j)$, quark $\to (i,0)$, anti-quark $\to (0,j)$, other $\to (0,0)$

$$\sum_{\sigma,\sigma'} A^*_\sigma \mathcal{C}_{\sigma,\sigma'} A_{\sigma'}$$

$$\mathcal{C}_{\sigma,\sigma'} \equiv \sum_{\{i\},\{j\}} \delta_{i_{\sigma_1},j_1}\delta_{i_{\sigma_2},j_2}\ldots\delta_{i_{\sigma_k},j_k}\delta_{i_{\sigma'_1},j_1}\delta_{i_{\sigma'_2},j_2}\ldots\delta_{i_{\sigma'_k},j_k} = N_c^{m(\sigma,\sigma')}$$

Colour-flow Feynman rules

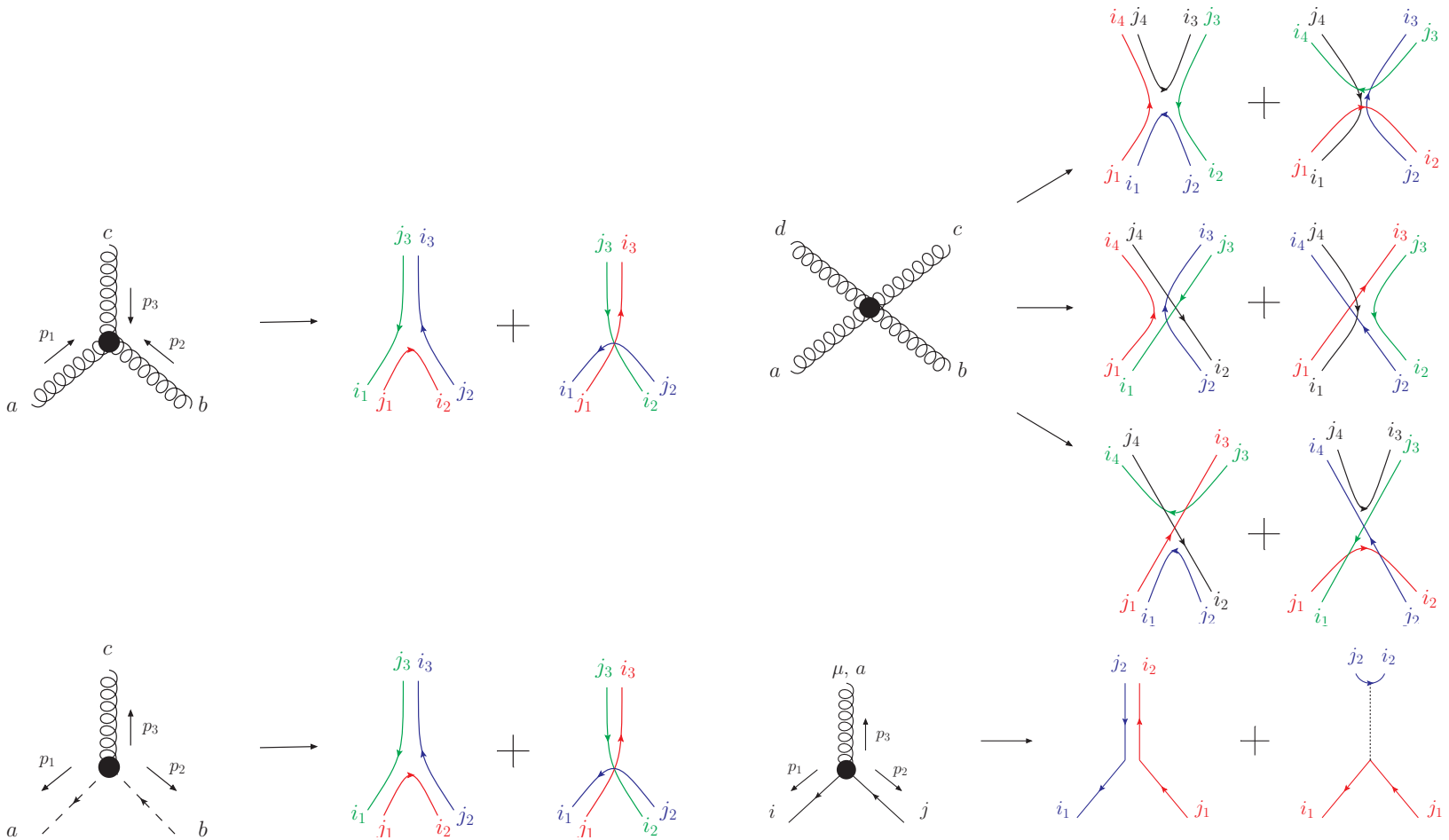

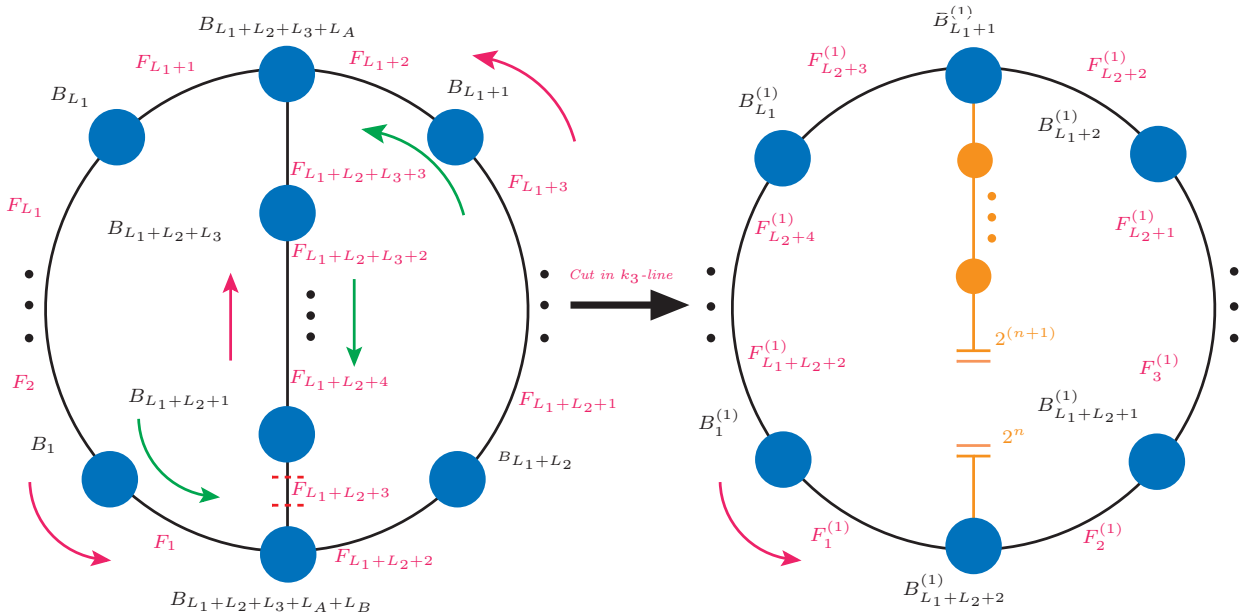
$B_{L_1+L_2+L_3+L_A}$
F_{L_1+1}
F_{L_1+2}
B_{L_1}
B_{L_1+1}
F_{L_1+3}
F_{L_1}
$F_{L_1+L_2+L_3+3}$
$B_{L_1+L_2+L_3}$
$F_{L_1+L_2+L_3+2}$
F_2
$F_{L_1+L_2+4}$
$B_{L_1+L_2+1}$
$F_{L_1+L_2+1}$
B_1
$B_{L_1+L_2}$
$F_{L_1+L_2+3}$
F_1
$F_{L_1+L_2+2}$
$B_{L_1+L_2+L_3+L_A+L_B}$
Cut in k_3-line
$\bar{B}^{(1)}_{L_1+1}$
$F^{(1)}_{L_2+3}$
$F^{(1)}_{L_2+2}$
$B^{(1)}_{L_1}$
$B^{(1)}_{L_1+2}$
$F^{(1)}_{L_2+4}$
$F^{(1)}_{L_2+1}$
$2^{(n+1)}$
$F^{(1)}_{L_1+L_2+2}$
$F^{(1)}_3$
$B^{(1)}_{L_1+L_2+1}$
$B^{(1)}_1$
2^n
$F^{(1)}_1$
$F^{(1)}_2$
$B^{(1)}_{L_1+L_2+2}$

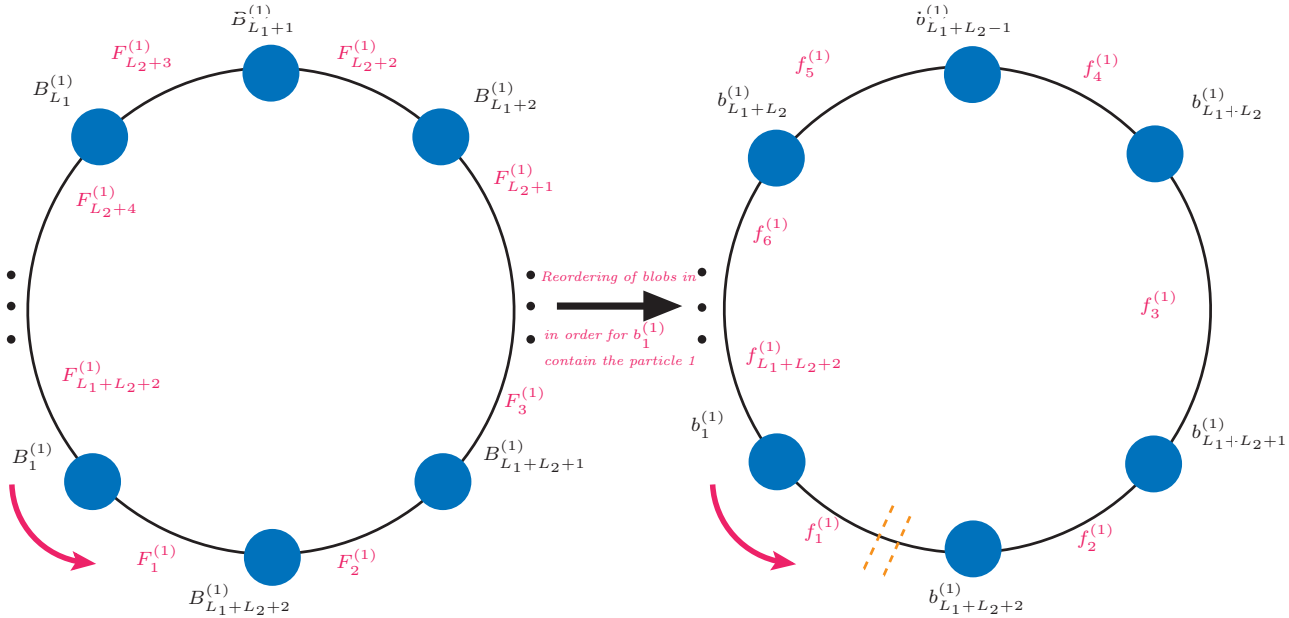
$\tilde{B}^{(1)}_{L_1+1}$
$F^{(1)}_{L_2+3}$
$F^{(1)}_{L_2+2}$
$B^{(1)}_{L_1}$
$B^{(1)}_{L_1+2}$
$F^{(1)}_{L_2+1}$
$F^{(1)}_{L_2+4}$
$F^{(1)}_{L_1+L_2+2}$
$F^{(1)}_{3}$
$B^{(1)}_{1}$
$B^{(1)}_{L_1+L_2+1}$
$F^{(1)}_{1}$
$F^{(1)}_{2}$
$B^{(1)}_{L_1+L_2+2}$
Reordering of blobs in
in order for $b^{(1)}_1$
contain the particle 1
$\dot{v}^{(1)}_{L_1+L_2-1}$
$f^{(1)}_{5}$
$f^{(1)}_{4}$
$b^{(1)}_{L_1+L_2}$
$b^{(1)}_{L_1+\cdot L_2}$
$f^{(1)}_{6}$
$f^{(1)}_{3}$
$f^{(1)}_{L_1+L_2+2}$
$b^{(1)}_{1}$
$b^{(1)}_{L_1+\cdot L_2+1}$
$f^{(1)}_{1}$
$f^{(1)}_{2}$
$b^{(1)}_{L_1+L_2+2}$

HELAC2LOOP@work

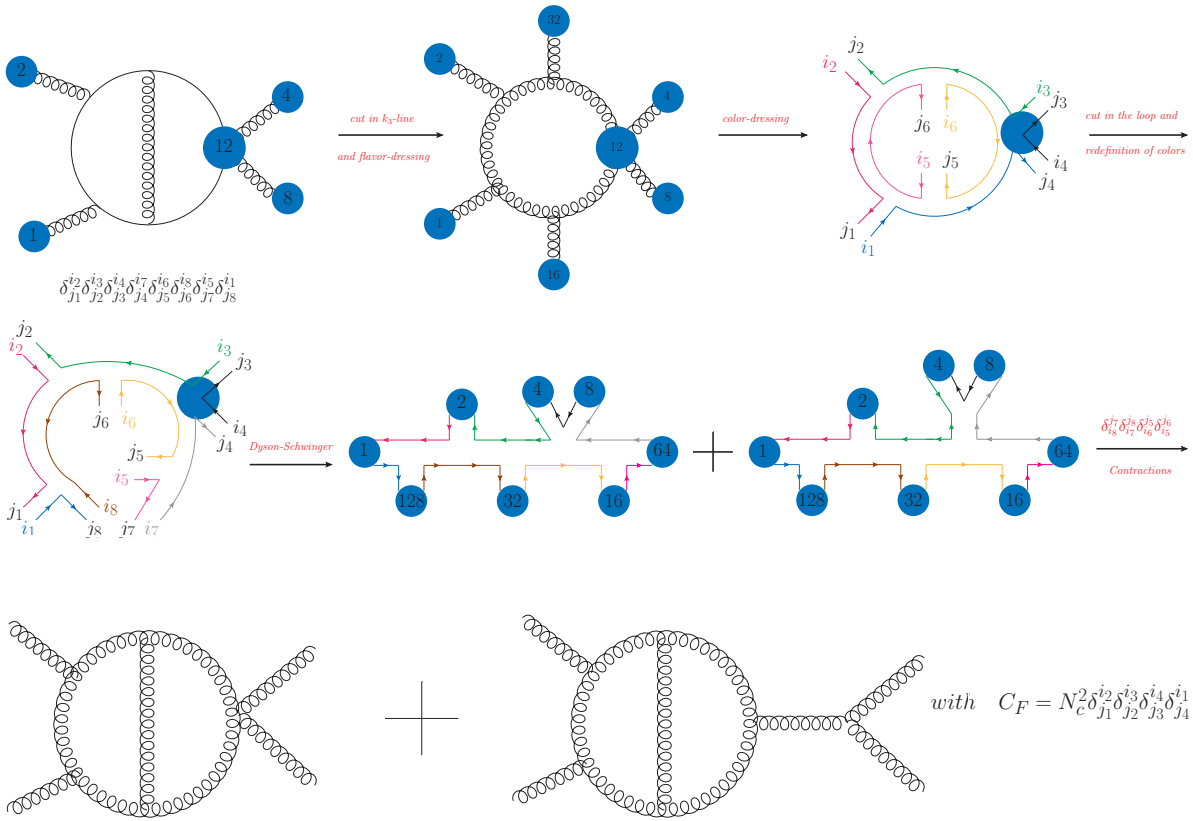

HELAC2LOOP@work

```
 INFO NUM         110  of          332          7
 INFO ====================================
INFO   4  80  35   9   1   1  16  35   5  64  35   7   0   0   0   0   1   2
INFO   4  12  35  10   1   1   4  35   3   8  35   4   0   0   0   0   1   1
INFO   4  92  35  11   1   2  12  35  10  80  35   9   0   0   0   0   1   1
INFO   5  92  35  11   2   2   4  35   3   8  35   4  80  35   9   0   1   5
INFO   4 124  35  12   1   1  32  35   6  92  35  11   0   0   0   0   1   2
INFO   4 126  35  13   1   1   2  35   2 124  35  12   0   0   0   0   1   1
INFO   4 254  35  14   1   1 128  35   8 126  35  13   0   0   0   0   1   2
INFO   6   1  12   1   2  12  35  35  35  35  35  35   0   0   0   0   5   9
```

Remark: Skeleton knows nothing about d: it can be used in $d = 4$ or any other dimension including $d = 4 - 2\epsilon$.

HELAC2LOOP@work

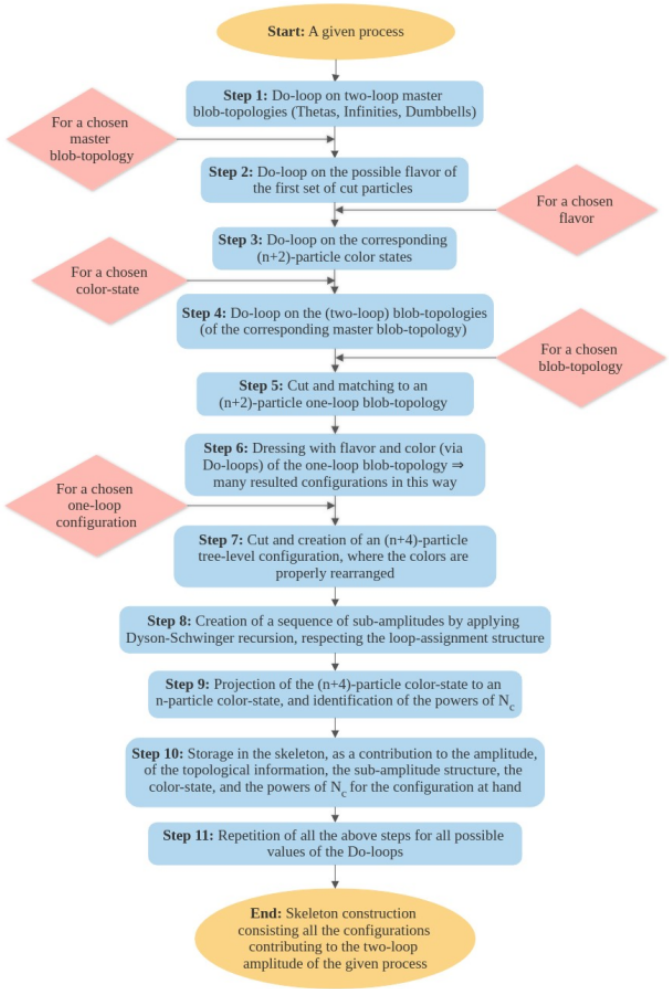

Process	#	*Loop-Flavors*	*Color*	*Size*	*Crea.Time*	*Nums*
$gg \to gg$	2	$\{g, c, \bar{c}\}$	Lead.	8.9 MB	15.017s	4560
$gg \to gg$	2	$\{g, q, \bar{q}, c, \bar{c}\}$	Full	110.6 MB	6m 54.574s	89392
$gg \to q\bar{q}$	2	$\{g, q, \bar{q}, c, \bar{c}\}$	Full	16.1 MB	3m 14.509s	13856
$gg \to ggg$	2	$\{g, c, \bar{c}\}$	Lead.	300.0 MB	21m 42.609s	81480
$gg \to q\bar{q}g$	2	$\{g, q, \bar{q}, c, \bar{c}\}$	Full	686.1 MB	400m 31.591s	318964
$gg \to gg$	1	$\{g, q, \bar{q}, c, \bar{c}\}$	Full	537.8 kB	2.386s	768
$gg \to ggg$	1	$\{g, q, \bar{q}, c, \bar{c}\}$	Full	15.1 MB	8m 53.349s	11496
$gg \to gggg$	1	$\{g, c, \bar{c}\}$	Lead.	394.0 MB	104m 14.95s	19680

TABLE: Table containing information for the skeleton of some QCD processes at one- and two-loop. Therein, the column # refers to the number of loops, ***Loop-Flavors*** denotes the flavor of the particles included in the loops, and ***Color*** indicates the color order, with Lead. and Full referring to leading- and full-color approximation, respectively. The columns ***Size*** and ***Crea.Time***, indicate the size of the skeleton and the real-time consumed for its construction, respectively. The last column (***Nums***) signifies the number of separate contributions (numerators) to the amplitude. These results have been obtained running 1-core on a laptop (i7 processor, 8-core, 24GB RAM).

Integrand reduction

→ Talk in GGI 2024: → click to link

A generic 2-loop integrand can be written using the following scalar product set:

$$\{p_i \cdot p_j, k_i \cdot k_j, k_i \cdot p_j, k_i \cdot \eta_j\}$$

$$\mathcal{R} = \frac{\mathcal{N}}{\mathcal{D}} = \frac{\sum_a c_a (z_1^{(a)})^{\beta_1} \dots (z_{n_a}^{(a)})^{\beta_N}}{D_1 \dots D_{N_p}}$$

where the z_i are any of the scalar products in the set.

Define $\bar{z}_i$ as the scalar products that cannot be eliminated by being written as linear combinations of D_i appearing in the denominator, known as irreducible scalar products (ISPs) and the transverse $k_i \cdot \eta_j$, if any.

$$\mathcal{N} = P_{max-cut} + \sum_i P_{n-to-max-cut} D_i + \sum_{ij} P_{n-n-to-max-cut} D_i D_j + \ldots$$

where all the P are polynomials in the so-called irreducible and transverse scalar products.

OPP@2L with HELAC

- Identify at each step the set of loop propagators we have to set to zero and solve the equations that put all of them on shell simultaneously (cut equations)
  For instance the 7-cut:

$$\left\{k_1.k_1 \to 0, k_1.k_2 \to 0, k_1.p_1 \to 0, k_1.p_2 \to -\frac{s}{2}, k_2.k_2 \to 0, k_2.p_2 \to \frac{s}{2} - k_2.p_1, k_2.p_3 \to -\frac{s}{2}\right\}$$

- Write the equations of the coefficients

$$N|_{cut} = \sum_i c_i m_i, \quad m_i = \prod \left(k_1 \cdot p_j\right)^{\alpha_{ij}} \left(k_2 \cdot p_j\right)^{\beta_{ij}} (k_1 \cdot \eta)^{\gamma_i} (k_2 \cdot \eta)^{\delta_i}$$

- Solve the system of equations for $\vec{c}$, subtract the on-shell expression from the original off-shell one, and move on to the next cut(s), where one less propagator is put on shell, AKA a sub-topology.
- Do this for all sub-topologies (usually up to 2 propagators ones for massless QCD), and the reduction is complete

OPP@2L with HELAC

This is an algebraic procedure that holds for any loop order.

- What do we expect at the end?

$$\mathcal{A} = \sum_i c_i F_i$$

c_i depends on the external world

F_i are Feynman integrals of the form

$$F_i \equiv F_{a_1 \ldots a_N} = \int d^d k \frac{\overbrace{(D_{m+1})^{a_{m+1}} \cdots (D_N)^{a_N}}^{ISP}}{\underbrace{(D_1)^{a_1} \cdots (D_m)^{a_m}}_{RSP}}$$

$$a_1, \ldots, a_m \to 1\ (2) \quad a_{m+1}, \ldots, a_N \to R_{cut} < R : \text{tensor rank}$$

that through IBP tables will be expressed in terms of Master Integrals.

$\to$ full numerical evaluation of pole and finite-remainder terms

2-Loop reduction example

Let's look at a specific $2 \to 2$ topology example, all gluons:

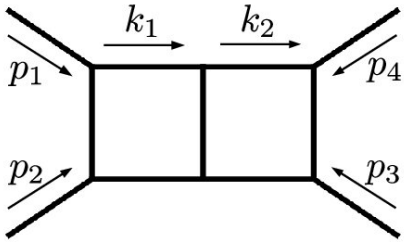

In $d = 4 - 2\epsilon$, there are 11 degrees of freedom: 8 from the components of 2 loop 4-momenta, and 3 for $\mu_{11}, \mu_{22}, \mu_{12}$ the ϵ part of k_1^2, k_2^2 and $k_1 \cdot k_2$ respectively.
With 7 cut equations, we have a remainder of 4 free parameters.
The right hand side of the OPP equation for the maximal cut has a total of 70 monomials, i.e. 70 coefficients to be fitted.
Use the 4 free parameters to get 70 sets of solutions in order to solve the system.

2-Loop reduction example

Challenge: Get a set of solutions to the cut equations which give an **M** matrix of rank 70.

Success! We have completed a Mathematica simulation of this fit, for all sub-topologies and get agreement with the known results from `Caravel`.

→ S. Abreu *et al.*, arXiv:2009.11957 [hep-ph].

2-Loop reduction example: 4-dimensions

In 4-dimensions, we begin with 8 degrees of freedom which we can use to construct solutions to the cut equations, so after imposing the on-shell condition only 1 parameter is left to build solutions with.
Problem!: Cut solution sets with 1 free parameter cannot generate a matrix of rank 70.
Success! In 4-dimensions though, we should use Gram determinant relations to reduce the number of coefficient we need to fit.

→ S. Badger, H. Frellesvig and Y. Zhang, JHEP **04** (2012), 055 [arXiv:1202.2019 [hep-ph]].

→ Y. Zhang, JHEP **09** (2012), 042 [arXiv:1205.5707 [hep-ph]].

Indeed after taking into account the Gram determinant relations we find 28 for the example of the $2 \to 2$ double-box maximal cut.
Completed a Mathematica simulation for the double-box and for all sub-topologies up to 2 propagators, as before.

OPP@2L with HELAC

- Amplitude reduction in 4 dimensions

- Cut equations $\rightarrow$ find systematically all solutions
- Integrand basis $\rightarrow$ systematically include gram-determinant relations
- R_1 terms $\rightarrow$ μ_{11}, μ_{12}, μ_{22}, 3 μ-parameters instead of one @1L
- R_2 terms

$\rightarrow$ S. Pozzorini, H. Zhang and M. F. Zoller, [arXiv:2001.11388 [hep-ph]].

$\rightarrow$ J. N. Lang, S. Pozzorini, H. Zhang and M. F. Zoller, [arXiv:2007.03713 [hep-ph]].

- $R \stackrel{?}{=} R_1 + R_2$

OPP@2L with HELAC

Amplitude reduction in $d = 4 - 2\epsilon$ requires reconstructing the dimensionally regulated numerator $\mathcal{N}$.

- Numerical Unitarity: gluing tree amplitudes in different integer dimensions $\rightarrow D_s$

$\rightarrow$ R. K. Ellis, W. T. Giele and Z. Kunszt, [arXiv:0708.2398 [hep-ph]].

$\rightarrow$ S. Abreu, F. Febres Cordero, H. Ita, M. Jaquier, B. Page and M. Zeng, [arXiv:1703.05273 [hep-ph]].

$\rightarrow$ S. Abreu, F. Febres Cordero, H. Ita, B. Page and V. Sotnikov, [arXiv:1809.09067 [hep-ph]].

$\rightarrow$ S. Abreu, J. Dormans, F. Febres Cordero, H. Ita, M. Kraus, B. Page, E. Pascual, M. S. Ruf and V. Sotnikov, [arXiv:2009.11957 [hep-ph]].

$\rightarrow$ V. Sotnikov, doi:10.6094/UNIFR/151540

- Introducing extra particles and Feynman rules

$\rightarrow$R. A. Fazio, P. Mastrolia, E. Mirabella and W. J. Torres Bobadilla, [arXiv:1404.4783 [hep-ph]].

Calculating the dimensionally regulated numerators with HELAC

$$\bar{q} = q + \tilde{q}, \quad \bar{\gamma}^{\mu} = \gamma^{\mu} + \tilde{\gamma}^{\mu}, \quad \bar{g}^{\mu\nu} = g^{\mu\nu} + \tilde{g}^{\mu\nu}$$

$$\mu = \tilde{q} \cdot \tilde{q} = \tilde{\not{q}}\tilde{\not{q}}$$

$$d - 4 = \tilde{g}^{\mu\nu}\tilde{g}_{\mu\nu} = \tilde{\gamma}^{\mu}\tilde{\gamma}_{\mu}$$

Back to one loop: how to compute

$$\tilde{N}\left(q, \tilde{q}^2, \epsilon\right)$$

HELAC aficionados:

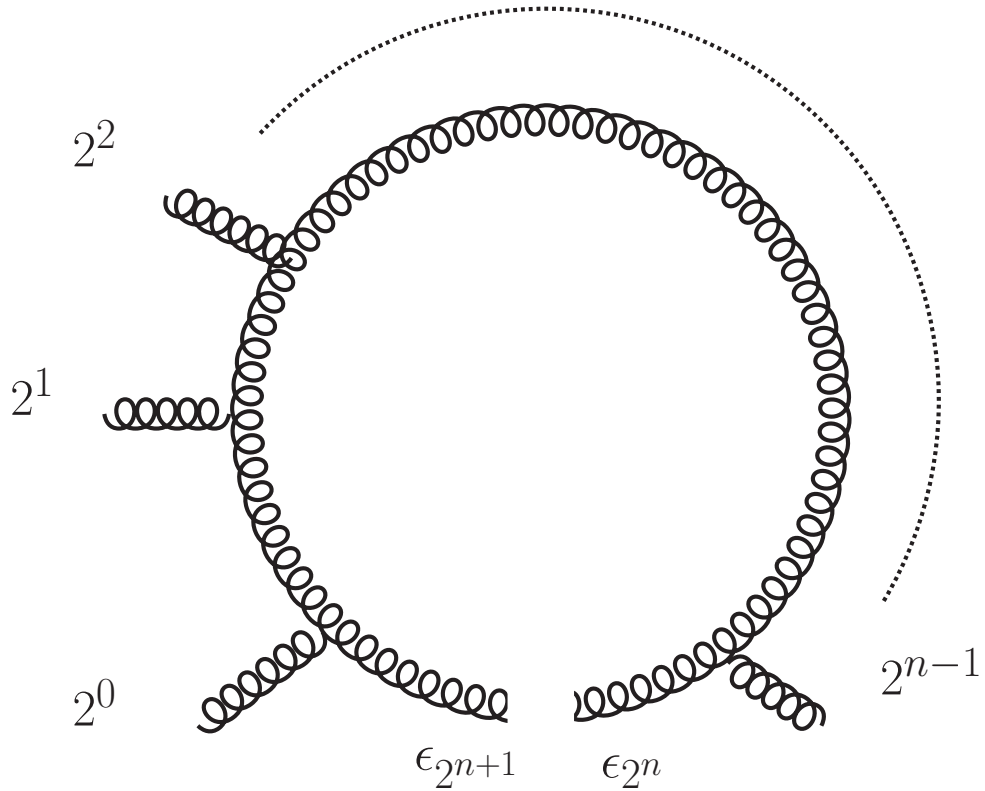

knowing that in the numerator:

$$q^2 X \to \mu X$$

$$\sum_{\lambda} \varepsilon_{L_1} \cdot \varepsilon_{L_2} X \to (d-4)\, X$$

$$\sum_{\lambda} (\varepsilon_{L_1} \cdot q)\, (\varepsilon_{L_2} \cdot q) X \to \mu X$$

to get X's from recursive equations ?

$$J_N^\mu,\ J_N\left[q\right],\ J_N\left[\varepsilon_{2^n}\right];\ J_N^\mu\left[\varepsilon_{2^n}\cdot q\right], Y_N\left[q\right]$$

satisfying the following recursive eqautions:

$$J_N^\mu = V^\mu\left(J_{N_1}, p_{N_1}; J_{N_2}, p_{N_2}\right) + \left(c_1 + 2c_2\right) J_{N_2}^\mu J_{N_1}\left[q\right]\mu$$

$$J_N\left[q\right] = \left(c_1 - c_2\right) J_{N_1}\cdot J_{N_2} - \left(2p_{N_1} + p_{N_2}\right)\cdot J_{N_2} J_{N_1}\left[q\right]$$

$$J_N\left[\varepsilon_{2^n}\right] = \begin{cases} -\left(2p_{N_1} + p_{N_2}\right)\cdot J_{N_2} J_{N_1}\left[\varepsilon_{2^n}\right] & N < 2^{n+2} - 2 \\ \left(p_{N_1} - p_{N_2}\right)^\mu J_{N_1}\left[\varepsilon_{2^n}\right] & N = 2^{n+2} - 2 \end{cases}$$

$$Y_N\left[q\right] = J_{N_1}\left[\varepsilon_{2^n}\cdot q\right]\cdot J_{N_2} - \left(2p_{N_1} + p_{N_2}\right)\cdot J_{N_2} Y_{N_1}\left[q\right]$$

where $p_{N_1} = c_1 q + p_{N_1,ext}$ and $p_{N_2} = c_2 q + p_{N_2,ext}$ and V represents the three-gluon vertex.

$$N\left(q,\tilde{q}^2,\epsilon\right) = J_{2^{n+2}-2}\cdot\varepsilon_1 + Y_{2^{n+1}-2}\left[q\right]\left(p_{2^{n+1}-2}-p_{2^{n+1}}\right)\cdot\varepsilon_1$$
$$-\left(J_{2^{n+1}-2}\left[\varepsilon_{2^n}\cdot q\right]\right)\cdot\varepsilon_1 + (d-4)\left(J_{2^{n+2}-2}\left[\varepsilon_{2^n}\right]\right)\cdot\varepsilon_1$$

Similar equations hold for all possible currents, including four-gluon vertices, quarks and ghosts. Details on the numerical reconstruction of the amplitude in $d = 4 - 2\epsilon$ dimensions will appear in a forthcoming publication.

OPP@2L with HELAC

- Implemented and tested for gluons, fermions and (anti-)ghosts running in the loop, for up to 6-gluon amplitudes
- Recursive equations for amplitudes with external fermion have been established $\rightarrow$ implementation & testing is underway
- Extending to two loops

Remark: Even the one-loop reduction is now different $\rightarrow$ no need to separately compute R_1 and R_2 terms.

Summary & Outlook

Current:

- Integrand construction @2L $\rightarrow$ solved and implemented
- Cut equations @2L: determining on-shell loop momenta $\rightarrow$ solved, implementation in progress
- Integrand basis construction and fitting @2L $\rightarrow$ solved, implementation in progress $\rightarrow$V. Sotnikov, doi:10.6094/UNIFR/151540
- $d = 4 - 2\epsilon \rightarrow$ implementation in progress for 1 loop

Near future:

- $d = 4 - 2\epsilon \rightarrow$ to be extended to 2 loops
- R_1 and R_2 terms @2L, if needed, and address $R \stackrel{?}{=} R_1 + R_2$.
- IBP reduction tables and MI numerical evaluation

$\rightarrow$ D. Chicherin and V. Sotnikov, JHEP **20** (2020), 167 $\rightarrow$D. Chicherin, V. Sotnikov and S. Zoia, JHEP **01** (2022), 096

Next-to-near future: automated 2-loop amplitude evaluation

Acknowledging

Thank you for your attention !

The research project was supported by the Hellenic Foundation for Research and Innovation (H.F.R.I.) under the 2nd Call for H.F.R.I. Research Projects to support Faculty Members & Researchers (Project Number: 2674).